Implementing quantum-logic operations, pseudopure states, and the Deutsch-Jozsa algorithm using noncommuting selective pulses in NMR

Kavita Dorai*
Department of Physics, Indian Institute of Science, Bangalore 560 012, India

Arvind†
Department of Physics, Guru Nanak Dev University, Amritsar 143 005, India

Anil Kumar‡
Department of Physics and Sophisticated Instruments Facility, Indian Institute of Science, Bangalore 560 012, India
(Received 9 June 1999; revised manuscript received 3 December 1999; published 15 March 2000)

We demonstrate experimentally the usefulness of selective pulses in NMR to perform quantum computation. Three different techniques based on selective pulse excitations have been proposed to prepare a spin system in a pseudopure state. We describe the design of ''portmanteau'' gates using the selective manipulation of level populations. A selective pulse implementation of the Deutsch-Jozsa algorithm for two and three-qubit quantum computers is demonstrated.

PACS number(s): 03.67.Lx, 76.60.−k

I. INTRODUCTION

The idea of exploiting the intrinsically quantum-mechanical nature of physical systems to perform computations has generated a lot of excitement recently [1,2]. Logical operations in quantum computation are implemented on quantum bits (qubits), where a qubit can be any quantum two-level system. The two eigenstates are mapped onto logical 0 and 1. While all classical computation can be performed using the above mapping, the fact that a qubit can exist in a general coherent superposition of logical states 0 and 1 leads to new possibilities for computation. The realization that computation can be performed reversibly [3,4] paved the way for the quantum-mechanical implementation of logic gates through unitary transformations [5,6]. The power of quantum computing lies in the fact that a single input state of a quantum computer can be a coherent superposition of all possible classical inputs. Consequently, algorithms that are intrinsically quantum in nature can be designed to solve problems hitherto deemed intractable on classical computers [7–9]. A major hurdle in achieving quantum computing experimentally is that of preserving quantum coherence while the computation is being performed, and the search for such ideal quantum systems yielded single charged ions confined in an ion trap [10] and nuclear spins in a liquid as possible choices.

It has been demonstrated that assemblies of nuclear spins in a liquid, which are largely isolated from their environment and have long relaxation times (so that coherence is retained for a while), can be used to build quantum information processors [1]. A system of N spins can exist in entangled quantum superposition states and can be thought of as an N-bit quantum computer. However, quantum computing requires pure states as inputs, whereas nuclear spins at thermal equilibrium are in a statistical mixture of pure states. It was demonstrated recently that it is possible to perform quantum computing with mixed-state ensembles rather than on an isolated system in a pure state [11]. This problem is circumvented by creating within the overall density matrix of the system, a subensemble that behaves like a pure state. Techniques to prepare such ''pseudopure'' states have been proposed by different groups [11–13]. Previous workers in the field employed various NMR methods like nonselective pulses, rf gradients, coherence transfer via J coupling, and simultaneous multisite excitation to create pseudopure states, construct universal logic gates, and implement quantum algorithms for two- and three-qubit systems [14–21].

In this paper, we explore the utility of transition- and spin-selective pulses, and exploit the noncommuting nature of operations on connected transitions to prepare a spin system in a pseudopure state, execute different logical operations simultaneously, and implement the Deutsch-Jozsa quantum algorithm on two- and three-qubit systems. The T_1 relaxation times in the molecules used, is of the order of a few seconds (3.4–4.6 sec), whereas T_2 relaxation occurs within an interval of around 1 sec. Selective excitation has been achieved using low-power, long-duration pulses of a rectangular shape. The length of these pulses is tailored to achieve sufficient selectivity in the frequency domain without perturbing the nearest line, and hence depends on the magnitude of the smallest J coupling present. The duration of the pulses applied varies from 100 to 263 ms (for J couplings of 9.55–3.8 Hz). For small computations, such as the ones performed here, drastic decoherence or dephasing does not occur during the duration of these selective pulses. However, the deleterious effects of such selective pulses must be considered and compensated for, whenever larger computations are attempted.

II. CREATION OF PSEUDOPURE STATES

The logical labeling technique to create pseudopure states is broadly categorized by the fact that unitary transforma-

*Electronic address: kavita@physics.iisc.ernet.in
†Electronic address: arvind@physics.iisc.ernet.in
‡Electronic address: anilnmr@physics.iisc.ernet.in

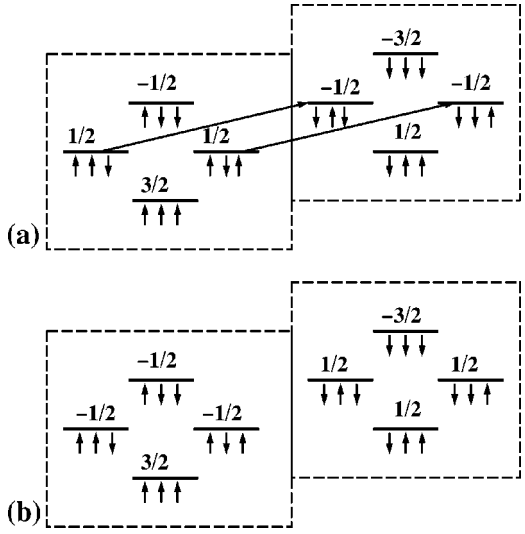

FIG. 1. The creation of a pseudopure state in an *AMX* three-spin system using logical labeling. (a) The population distribution of the thermal equilibrium state. (b) The population distribution of a pseudopure state, created by inverting the populations of the two single-quantum *A* transitions shown in (a) by long arrows.

tions are used to redistribute the populations of states, such that an effective pure state is obtained in the submanifold of qubits (spins) to be used for computation, and ancillary qubits are used as ''labels.'' While the concept underlying the logical labeling method of pseudopure state creation was delineated by Chuang and co-workers [13,16], there have been very few experimental implementations of such an elegant technique [21]. We have designed a few pulse schemes using transition-selective pulses to create such logically labeled pseudopure states. Consider a three-spin-1/2 system(*AMX*), with energy levels labeled as in Fig. 1. The selective inversion of two unconnected single-quantum transitions of the *A* spin ($|\uparrow\uparrow\downarrow\rangle\rightarrow|\downarrow\uparrow\downarrow\rangle$ and $|\uparrow\downarrow\uparrow\rangle\rightarrow|\downarrow\downarrow\uparrow\rangle$) would lead to the creation of a logically labeled pseudopure state, with *A* being the ''label qubit'' and *M* and *X* being the ''work qubits'' available for computation. The first four eigenstates (labeled by the first spin being in the $|\uparrow\rangle$ state) now form a manifold that corresponds to a two-qubit pseudopure state, while the last four (labeled by the first spin being in the $|\downarrow\rangle$ state) form a separate manifold that corresponds to another two-qubit pseudopure state. The creation of a pseudopure state by this method leads to relative population differences of

$$\begin{array}{cccccccc} \uparrow\uparrow\uparrow & \uparrow\uparrow\downarrow & \uparrow\downarrow\uparrow & \uparrow\downarrow\downarrow & \downarrow\uparrow\uparrow & \downarrow\uparrow\downarrow & \downarrow\downarrow\uparrow & \downarrow\downarrow\downarrow \\ 3/2 & -1/2 & -1/2 & -1/2 & 1/2 & 1/2 & 1/2 & -3/2. \end{array} \tag{2.1}$$

Homonuclear three-spin case: The experimental creation of a logically labeled pseudopure state in the homonuclear three-spin system of 2,3 dibromopropionic acid is shown in Fig. 2. The pseudopure state has been distilled by manipulating unconnected single quantum transitions of the label qubit *A*, as detailed in Eq. (2.1). The transition-selective π pulses were applied on the two central (nearly overlapping) transitions of the *A* spin.

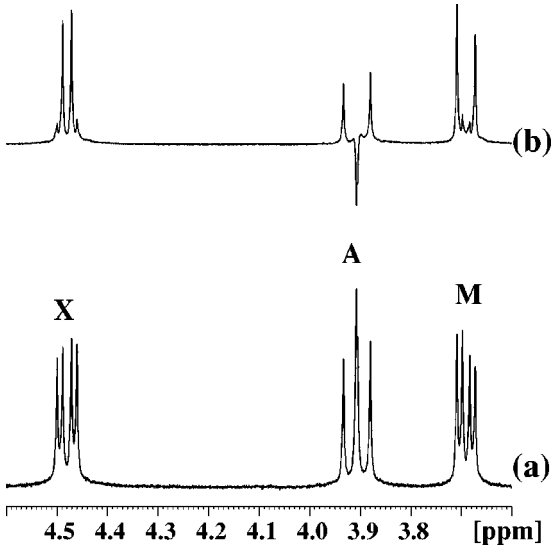

FIG. 2. A logically labeled pseudopure state in the homonuclear three-spin system (*AMX*) of 2,3 dibromopropionic acid. (a) The equilibrium proton spectrum is shown, with the three protons labeled *A*, *M*, and *X* resonating at $\delta_A = 3.91$ ppm, $\delta_M = 3.69$ ppm, and $\delta_X = 4.48$ ppm, respectively. (b) The selective inversion of the two (nearly overlapping) central transitions of the *A* spin leads to the creation of a logically labeled pseudopure state, which has been read by a small flip angle (10°) detection pulse. Long, low-power rectangular pulses have been used for selective excitation.

Heteronuclear three-spin case: The experimental creation of a logically labeled pseudopure state in the heteronuclear three spin system of 4-fluoro,7-nitro benzofurazan is shown in Fig. 3. Two selective π pulses were applied on the central, nearly overlapping unconnected single-quantum transitions ($|\uparrow\uparrow\downarrow\rangle\rightarrow|\downarrow\uparrow\downarrow\rangle$ and $|\uparrow\downarrow\uparrow\rangle\rightarrow|\downarrow\downarrow\uparrow\rangle$) of the *A* spin (the proton in this case). The *A* spin is the ''label'' qubit and the other two spins (the third spin being fluorine in this case) are the ''work'' qubits. It is to be noted that the spectral pattern of the *X* spin in the two pseudopure states created in the homonuclear and heteronuclear systems are mirror images of each other, i.e., intensities of (0,2,2,0) are obtained for the *X* spin in Fig. 2(b), while the *X* spin multiplet pattern is (2,0,0,2) in Fig. 3. This difference reflects the relative sign of the coupling constants in these systems. Heteronuclear ^{19}F-^{1}H spin systems are useful for quantum computing, as they have the twin advantages of good sensitivity and long relaxation times.

Other methods to implement a logically labeled pseudopure state can be designed, based on the selective manipulation of the populations of multiple quanta. For instance, the inversion of the double quantum $|\downarrow\uparrow\uparrow\rangle\rightarrow|\downarrow\downarrow\downarrow\rangle$, followed by the inversion of the single quantum transition $|\uparrow\downarrow\downarrow\rangle\rightarrow|\downarrow\downarrow\downarrow\rangle$, leads to another pseudopure state. The redistribution of equilibrium populations leads to relative population differences for the pseudopure state

$$\begin{array}{cccccccc} \uparrow\uparrow\uparrow & \uparrow\uparrow\downarrow & \uparrow\downarrow\uparrow & \uparrow\downarrow\downarrow & \downarrow\uparrow\uparrow & \downarrow\uparrow\downarrow & \downarrow\downarrow\uparrow & \downarrow\downarrow\downarrow \\ 3/2 & 1/2 & 1/2 & 1/2 & -3/2 & -1/2 & -1/2 & -1/2. \end{array} \tag{2.2}$$

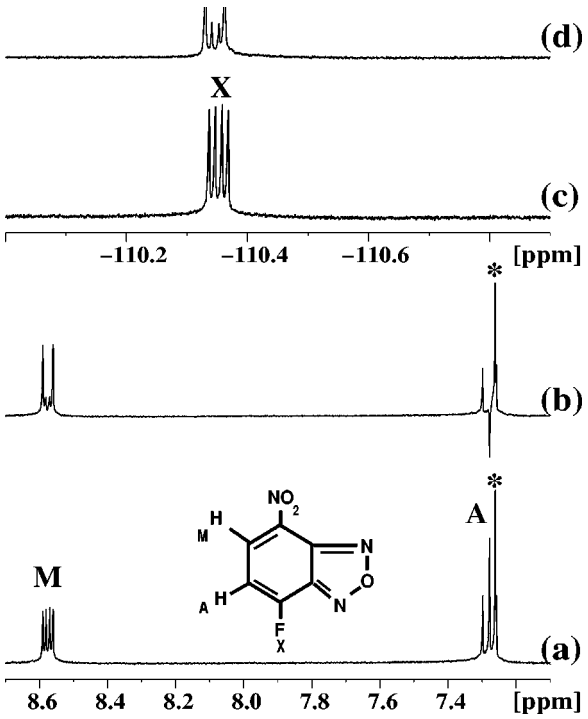

FIG. 3. The creation of a logically labeled pseudopure state in a 4-fluoro,7-nitro benzofurazan (*AMX* system). Transition-selective π pulses have been applied on the two overlapping central transitions of the ''label'' qubit (proton A). The asterisk labels the solvent peak. The normal proton and fluorine spectra are shown in (a) and (c) with the spins resonating at $\delta_A = 7.28$ ppm, $\delta_M = 8.57$ ppm, and $\delta_X = -110.35$ ppm, respectively. The proton and fluorine spectra corresponding to the pseudopure state are shown in (b) and (d), respectively, with the ''work'' qubits M and X being in a logically labeled pseudopure state. The state of the system has been monitored by a small flip angle detection pulse.

Experimentally, the double quantum can be inverted by a cascade of π pulses on progressively connected single quantum transitions [22]. The inversion of the single quantum transition $|\downarrow\uparrow\uparrow\rangle \rightarrow |\downarrow\uparrow\downarrow\rangle$, followed by the inversion of the zero quantum $|\uparrow\downarrow\downarrow\rangle \rightarrow |\downarrow\uparrow\downarrow\rangle$, leads to yet another pseudopure state. The redistribution of equilibrium populations leads to the relative population differences

$$\begin{array}{cccccccc} \uparrow\uparrow\uparrow & \uparrow\uparrow\downarrow & \uparrow\downarrow\uparrow & \uparrow\downarrow\downarrow & \downarrow\uparrow\uparrow & \downarrow\uparrow\downarrow & \downarrow\downarrow\uparrow & \downarrow\downarrow\downarrow \\ 3/2 & 1/2 & 1/2 & 1/2 & -1/2 & -1/2 & -1/2 & -3/2. \end{array} \tag{2.3}$$

Experimentally, the zero quantum can be inverted by a cascade of π pulses on two regressively connected single quantum transitions by the cascade $\pi^{1,2}\pi^{1,3}\pi^{1,2}$(spectra not shown) [22].

The state of the system after the creation of the logically labeled pseudopure state has been read out by a small flip angle detection pulse in each case. While it is usual in quantum computing to use pulses of flip angle 90° for the readout operation, this will not provide a useful output for logical labeling experiments. To illustrate this point, consider a logically labeled pseudopure state for the three-spin *AMX* system, with A being the label qubit, and M and X the work qubits [Eq. (2.1)]. The traceless, deviation density matrix corresponding to this pseudopure state can be described in terms of product operators (which are just products of spin angular momentum operators)

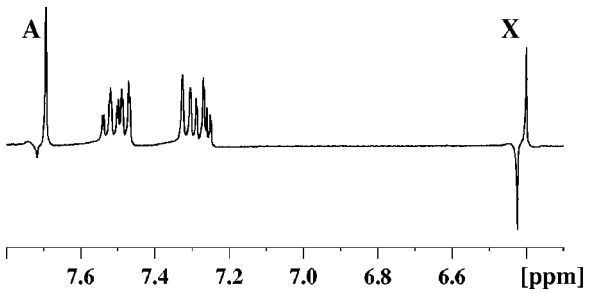

FIG. 4. The logical SWAP operation implemented on the two-spin system of Coumarin. The result of the application of a $[\pi]_x$ pulse on one of the X transitions, followed by a $[\pi]_x$ pulse on the regressively connected A transition is shown, which corresponds to a logical SWAP on the nonequilibrium state of the spin system. A small angle (10°) read pulse has been used. The one-dimensional spectrum and structure of Coumarin are shown in Fig. 5.

$$\sigma_{p\text{-}pure} = M_z + X_z + 4A_z M_z X_z . \tag{2.4}$$

A detection pulse of flip angle α leads to the NMR observable terms

$$(M_x + X_x)\sin\alpha + (4A_x M_z X_z + 4A_z M_x X_z + 4A_z M_z X_x) \times \cos^2\alpha \sin\alpha. \tag{2.5}$$

Hence a 90° detection pulse would not be able to read out all the product operators present in the density matrix [Eq. (2.4)], and a small-angle read pulse is required.

III. QUANTUM LOGIC GATES

We now proceed toward the implementation of quantum logic gates using NMR [11,18]. The two-qubit quantum XOR (or controlled-NOT) gate has been demonstrated to be fundamental for quantum computation [5] and has been implemented in NMR by a selective $[\pi]_x$ pulse on a single transition [11]. It has been proved that the reversible quantum XOR gate, supplemented by a set of general one-qubit quantum gates, is sufficient to perform any arbitrary quantum computation [5]. Hence, with the achievement of the experimental implementation of the XOR and one-qubit gates in NMR, it does not seem necessary to look for the design and construction of other gates. Nevertheless, it is important in terms of complexity in large circuits and ease of experimental implementation, to look toward the design of efficient logic networks. In this direction, gates that achieve the implementation of two or more logic operations simultaneously would be useful in reducing computational time in circuits that require a large number of logical operations. We detail the design and experimental implementation of such gates here; borrowing from Lewis Carroll, we call such ''many-in-one'' gates ''Portmanteau'' gates [23].

The logical SWAP *operation*: Consider a two-spin system

(*AX*) with each spin being a qubit, the spin *A* being the first qubit and the spin *X* the second qubit. The eigenstates of this system can be represented by $|\epsilon_1,\epsilon_2\rangle$, where ϵ_1 and ϵ_2 are 0 or 1. The logical SWAP operation completely exchanges the states of a pair of qubits, from $|\epsilon_1,\epsilon_2\rangle$ to $|\epsilon_2,\epsilon_1\rangle$, the unitary transformation corresponding to such an operation being

$$U_{\mathrm{SWAP}}=\begin{bmatrix}1&0&0&0\\0&0&1&0\\0&1&0&0\\0&0&0&1\end{bmatrix}. \tag{3.1}$$

This gate might be useful during the course of a computation when qubits need to be permuted [18]. In spin systems where some scalar *J* couplings are ill resolved, the logical SWAP could be used to compensate for the missing couplings [20].

Madi *et al.* [20] implemented the SWAP operation using an INEPT-type sequence, with nonselective rf pulses and *J* evolution. It is interesting to note that the logical SWAP operation can be achieved by selectively interchanging the populations of the zero quantum levels. Since these levels are not connected by single-quantum transitions, the population exchange will have to be achieved indirectly.

The inversion of the zero quantum (SWAP) requires a cascade of three selective π pulses on regressively connected transitions, for example, $[\pi]_x^{A_1}[\pi]_x^{X_1}[\pi]_x^{A_1}$ [22]. Since this would lead to the same spectrum as the equilibrium spectrum, a nonequilibrium state has been first created by preceding the cascade with a selective $[\pi]_x^{A_1}$ pulse, yielding the cascade $[\pi]_x^{A_1}[\pi]_x^{X_1}[\pi]_x^{A_1}[\pi]_x^{A_1}=[\pi]_x^{A_1}[\pi]_x^{X_1}$. This amounts to the execution of a logical SWAP operation on a nonequilibrium state. The experimental implementation of this operation is shown in Fig. 4 on the two spin system of Coumarin.

We now explore the implementation of gates that realize various combinations of the SWAP, XOR (XNOR), and NOT operations. The action and matrix representations of the XOR, XNOR, and NOT gates (all with their outputs on the first qubit) are given by

$$|\epsilon_1,\epsilon_2\rangle \xrightarrow{\mathrm{XOR}} |\epsilon_1\oplus\epsilon_2,\epsilon_2\rangle,\quad U^1_{\mathrm{XOR}}=\begin{bmatrix}1&0&0&0\\0&0&0&1\\0&0&1&0\\0&1&0&0\end{bmatrix},$$

$$|\epsilon_1,\epsilon_2\rangle \xrightarrow{\mathrm{XNOR}} |\overline{\epsilon_1\oplus\epsilon_2},\epsilon_2\rangle,\quad U^1_{\mathrm{XNOR}}=\begin{bmatrix}0&0&1&0\\0&1&0&0\\1&0&0&0\\0&0&0&1\end{bmatrix}, \tag{3.2}$$

$$|\epsilon_1,\epsilon_2\rangle \xrightarrow{\mathrm{NOT}} |\overline{\epsilon_1},\epsilon_2\rangle,\quad U^1_{\mathrm{NOT}}=\begin{bmatrix}0&0&1&0\\0&0&0&1\\1&0&0&0\\0&1&0&0\end{bmatrix}.$$

The superscript 1 indicates that the output of the gate is obtained on the first qubit. The matrices U^2_{XOR}, etc., corresponding to the output on the second qubit, can be similarly constructed.

Logical SWAP+XOR(XNOR): The execution of a logical SWAP operation followed by an XOR gate (with its output on the first qubit), can be defined through its action on $|\epsilon_1,\epsilon_2\rangle$, and leads to the final state $|\epsilon_1\oplus\epsilon_2,\epsilon_1\rangle$(or to $|\overline{\epsilon_1\oplus\epsilon_2},\epsilon_1\rangle$ for a SWAP followed by an XNOR gate with its output on the first qubit), with their explicit matrix representations being

$$U_{\mathrm{SWAP}+XOR}=U^1_{\mathrm{XOR}}U_{\mathrm{SWAP}}=\begin{bmatrix}1&0&0&0\\0&0&0&1\\0&1&0&0\\0&0&1&0\end{bmatrix},$$

$$U_{\mathrm{SWAP}+\mathrm{XNOR}}=U^1_{\mathrm{XNOR}}U_{\mathrm{SWAP}}=\begin{bmatrix}0&1&0&0\\0&0&1&0\\1&0&0&0\\0&0&0&1\end{bmatrix}. \tag{3.3}$$

An implementation of these operations requires the application of selective $[\pi]_x$ pulses consecutively on two regressively connected transitions, and the resulting spectrum on two bits is identical to Fig. 4.

XOR(XNOR)+*logical* SWAP+NOT: The implementation of an XOR gate (with the output on the first qubit), followed by a SWAP operation and then a NOT gate on the first qubit, corresponding to a final state of $|\overline{\epsilon_2},\epsilon_1\oplus\epsilon_2\rangle$, can be experimentally achieved by transition-selective $[\pi]_x$ pulses applied consecutively on two progressively connected transitions. Reversing the order of application of the pulses leads to the final state $|\overline{\epsilon_1\oplus\epsilon_2},\overline{\epsilon_1}\rangle$ which corresponds to an XNOR +*logical* SWAP+NOT gate, with the output on the second qubit.

These gates correspond to the unitary matrices given by

$$U_{\mathrm{XOR}+\mathrm{SWAP}+\mathrm{NOT}}=U^1_{\mathrm{NOT}}U_{\mathrm{SWAP}}U^1_{\mathrm{XOR}}=\begin{bmatrix}0&0&0&1\\0&1&0&0\\1&0&0&0\\0&0&1&0\end{bmatrix}, \tag{3.4}$$

$$U_{\mathrm{XNOR}+\mathrm{SWAP}+\mathrm{NOT}}=U^2_{\mathrm{NOT}}U_{\mathrm{SWAP}}U^2_{\mathrm{XNOR}}=\begin{bmatrix}0&0&1&0\\0&1&0&0\\0&0&0&1\\1&0&0&0\end{bmatrix}.$$

The experimental implementation of such gates is shown in Figs. 5(b) and 5(c). It is interesting to note that these operations do not commute, so the order in which the pulses are applied is important and its reversal leads to different logical operations.

NOT+*logical* SWAP: The NOT gate followed by a logical SWAP operation on two qubits (or vice versa, since these

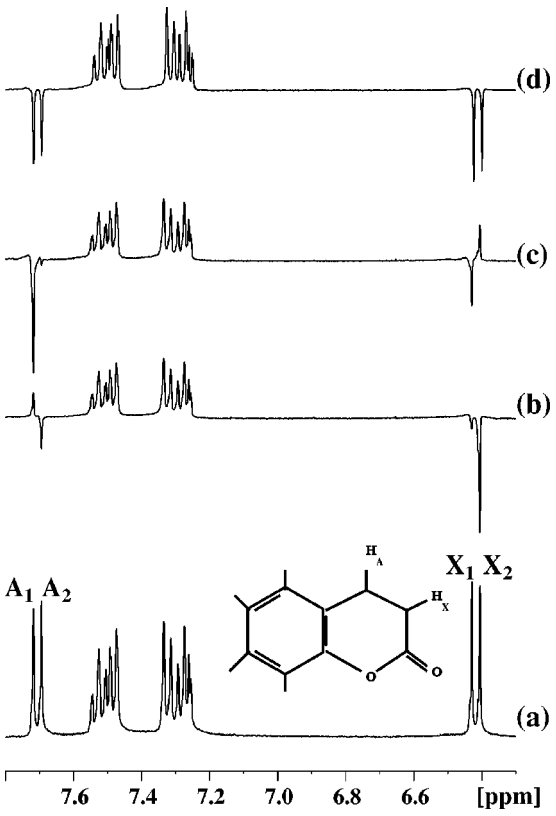

FIG. 5. The experimental implementation of various portmanteau gates. (a) Reference spectrum of Coumarin at thermal equilibrium. (b) The implementation of an $XOR+SWAP+NOT$ (by the pulse cascade $[\pi]_x^{A_1}$ followed by $[\pi]_x^{X_2}$, where A_1 and X_2 refer to progressively connected transitions of spins A and X, respectively). (c) The implementation of an XNOR+SWAP+NOT ($[\pi]_x^{X_2}$ followed by $[\pi]_x^{A_1}$). (d) The implementation of a NOT+SWAP ($[\pi]_x^{A_1}[\pi]_x^{X_2}[\pi]_x^{A_1}$). The state of the spin system is read by a small (10°) angle pulse in each case.

operations commute) leads to $|\bar{\epsilon}_2,\bar{\epsilon}_1\rangle$ when applied to the state $|\epsilon_1,\epsilon_2\rangle$. This action suffices to determine the unitary matrix for the above operation, given by

$$U_{\mathrm{NOT+SWAP}}=U_{\mathrm{SWAP}}U_{\mathrm{NOT}}=U_{\mathrm{NOT}}U_{\mathrm{SWAP}}=\begin{bmatrix}0&0&0&1\\0&1&0&0\\0&0&1&0\\1&0&0&0\end{bmatrix}. \tag{3.5}$$

The experimental implementation has been achieved by selectively inverting the populations of the double-quantum levels. A cascade of transition-selective $[\pi]_x$ pulses has been applied on two progressively connected transitions [Fig. 5(d)].

The implementation of various portmanteau gates on a thermal initial state is shown in Fig. 5 for the two-spin system of Coumarin. The same pulse schemes are expected to implement the above logic operations on other initial states (for instance, a pseudopure or a coherent superposition of states) as well. As an illustration, consider the portmanteau gate XOR+SWAP+NOT. The unitary matrix corresponding to it [Eqn. (3.4)] can be decomposed into two matrices

$$U_{\mathrm{XOR+SWAP+NOT}}=U_{\pi_x}^{X_2}U_{\pi_x}^{A_1},$$

$$U_{\pi_x}^{A_1}=\begin{bmatrix}1&0&0&0\\0&1&0&0\\0&0&0&i\\0&0&i&0\end{bmatrix},\quad U_{\pi_x}^{X_2}=\begin{bmatrix}0&0&i&0\\0&1&0&0\\i&0&0&0\\0&0&0&1\end{bmatrix}. \tag{3.6}$$

The matrices $U_{\pi_x}^{A_1}$ and $U_{\pi_x}^{X_2}$ correspond to selective $[\pi]_x$ pulses on the A_1 and X_2 transitions, respectively. A low-power, long duration rectangular pulse is applied to achieve the desired selectivity. These transition-selective pulses can be expanded in terms of single-transition operators (the expansion is independent of the state of the spin system [22,24]). This realization in terms of single transition operators is valid when the power of the rf pulse is low compared to the the J coupling and the chemical shift difference between the spins ($w_1 \ll 2\pi J \ll \delta_{AX}$). One is thus able to realize the unitary transformations required to implement the desired logical operations, without prior knowledge of the state of the system. However as noted recently [25], a more complete Hamiltonian description might be required to describe evolution under selective pulses, in order to fully establish the generality of the above schemes.

It is to be noted that we have used selective pulses polarized along the x direction. The phases of the pulses are important, and have been experimentally ensured by appropriate phase cycling schemes.

IV. IMPLEMENTATION OF THE DEUTSCH-JOZSA QUANTUM ALGORITHM

Finally, we experimentally implement the Deutsch-Jozsa (DJ) algorithm using selective pulses. The DJ algorithm determines whether an unknown function $f(x)$ is constant or balanced [8]. In the simplest version, $f(x)$ is a mapping from a single bit to a single bit and the function is constant if $f(x)$ is independent of x and it is balanced if $f(x)$ is zero for one value of x and unity for the other value. The generalization to N bits is conceptually simple, and $f(x)$ in this case is constant if it is independent of x and balanced if it is zero for half the values of x and unity for the other half. A classical computer proceeding deterministically would require up to $2^{N-1}+1$ function calls to check if $f(x)$ is constant or balanced; even if half the inputs have been evaluated and all outputs have been found to be 0 (or 1) one cannot conclude that the function is constant. The quantum version of the algorithm determines if the function is balanced or constant using only a *single* function call. For the one-bit case this is achieved by evaluating the value of $f(0)\oplus f(1)$ (where $\oplus$ denotes addition modulo 2). The binary function f is encoded in a unitary transformation by the propagator U_f by including an extra input qubit such that

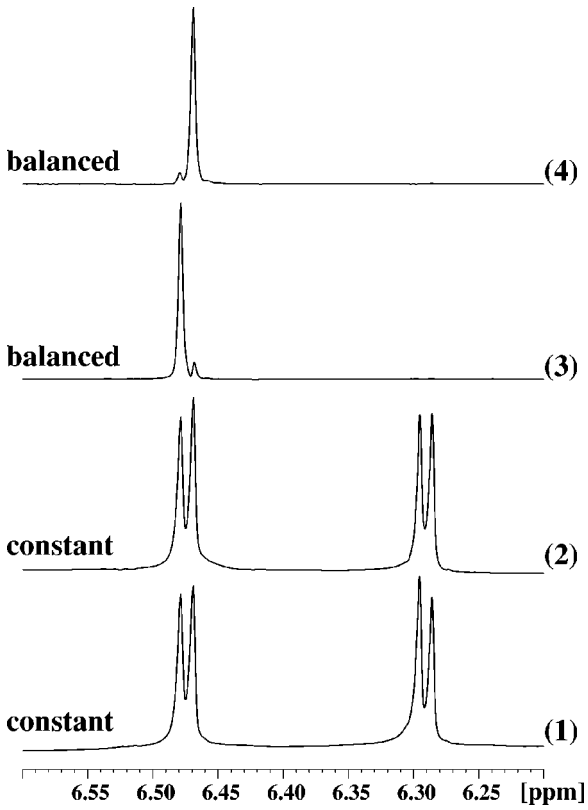

FIG. 6. A selective pulse implementation of the DJ quantum algorithm on a two-qubit system 5-nitro furaldehyde, at room temperature on a 400-MHz spectrometer. The results after applying the unitary transformations U_1, U_2, U_3, and U_4 on a coherent superposition are shown in traces (1)–(4), respectively.

$$|x\rangle|y\rangle \xrightarrow{U_f} |x\rangle|y \oplus f(x)\rangle.$$

The four possible functions for the single-bit DJ algorithm are categorized as

	Const.		Bal.	
x	f_1	f_2	f_3	f_4
0	0	1	0	1
1	0	1	1	0

The unitary transformations corresponding to the four possible propagators U_f can be easily constructed:

$$U_1 = \begin{bmatrix} 1 & 0 & 0 & 0 \\ 0 & 1 & 0 & 0 \\ 0 & 0 & 1 & 0 \\ 0 & 0 & 0 & 1 \end{bmatrix} \quad U_2 = \begin{bmatrix} 0 & 1 & 0 & 0 \\ 1 & 0 & 0 & 0 \\ 0 & 0 & 0 & 1 \\ 0 & 0 & 1 & 0 \end{bmatrix},$$
$$U_3 = \begin{bmatrix} 1 & 0 & 0 & 0 \\ 0 & 1 & 0 & 0 \\ 0 & 0 & 0 & 1 \\ 0 & 0 & 1 & 0 \end{bmatrix} \quad U_4 = \begin{bmatrix} 0 & 1 & 0 & 0 \\ 1 & 0 & 0 & 0 \\ 0 & 0 & 1 & 0 \\ 0 & 0 & 0 & 1 \end{bmatrix}. \tag{4.1}$$

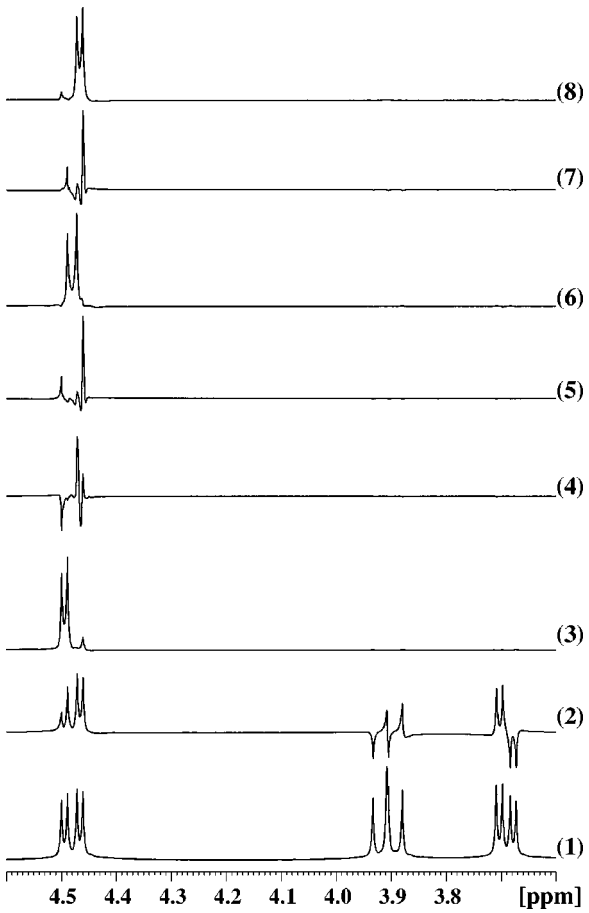

FIG. 7. Selective pulse implementation of the DJ algorithm on the three-qubit system of 2,3 dibromopropionic acid. The two constant functions f_1 and f_2 are shown in Eqs. (2.1) and (2.2), respectively, while the unitary transforms corresponding to the balanced functions f_3–f_8 are implemented in traces (3)–(8), respectively.

The algorithm requires one input spin and one work spin. Using the propagator U_f and appropriate input states, one can proceed with the implementation of the algorithm. Previous workers in the field [14,17], used a combination of spin-selective ($\pi/2$) pulses and evolution under the scalar coupling J, to encode the DJ algorithm on a two-qubit quantum computer.

We have implemented the DJ algorithm using spin- and transition-selective π pulses. The experiment begins with both qubits in a superposition of states, achieved by a nonselective $[\pi/2]_y$ pulse on both spins. After application of the propagators U_i, the first qubit (the ''control'' qubit) remains in the superposition state while the desired result $[f(0) \oplus f(1)]$ is encoded as the appearance or disappearance of the lines of the target qubit. The U_1 transformation corresponds to the unity operation or ''do nothing,'' while the U_2 transform is achieved by a spin-selective $[\pi]_x$ pulse on the control qubit. The U_3 and U_4 transformations are implemented by selective π pulses on the $|{\downarrow}{\uparrow}\rangle \rightarrow |{\downarrow}{\downarrow}\rangle$ and the $|{\uparrow}{\uparrow}\rangle \rightarrow |{\uparrow}{\downarrow}\rangle$ transitions, respectively.

The implementation of this algorithm does not require pure initial states, as similar results can be read out from the spectrum if one starts with thermal initial states instead. In a

single measurement, one can distinguish between constant and balanced functions on the basis of the disappearance of the lines of the target qubit in the spectrum. These predictions are borne out by the experimental spectra in Fig. 6. The phase of the transition-selective pulse (to implement U_3 and U_4) has been stepped through $(x,-x,y,-y)$ to suppress phase distortions, and leads to the total suppression of the target qubit lines and the retention of only one line of the control qubit.

The algorithm to distinguish between the two categories (constant or balanced) of two-bit binary functions is implemented on a three-qubit NMR computer, by evaluating $|x\rangle|y\rangle|z\rangle \xrightarrow{U_f} |x\rangle|y\rangle|z\oplus f(x,y)\rangle$. The eight possible (two constant and six balanced) two-bit binary functions are categorized as

		Const.		Bal.					
x	y	f_1	f_2	f_3	f_4	f_5	f_6	f_7	f_8
0	0	0	1	0	1	1	0	1	0
0	1	0	1	0	1	0	1	0	1
1	0	0	1	1	0	1	0	0	1
1	1	0	1	1	0	0	1	1	0

Previous researchers used shaped pulses generated by an rf wave form generator to implement the two-bit DJ algorithm using three qubits; the pulse wave forms were tailored to selectively excite two or more frequencies simultaneously [19].

Here we describe a selective pulse implementation of the DJ algorithm using simple rectangular pulses (Fig. 7). These low-power, long-duration transition-selective pulses are applied consecutively, and do not require any special hardware for their application. The unitary transforms have been implemented on a coherent superposition of all three qubits, achieved by a nonselective $\pi/2$ pulse on a thermal initial state. The two constant functions f_1 and f_2 correspond to the unity operation and a spin-selective $[\pi]_x$ pulse on the multiplet of the control qubit, respectively. The unitary transformations encoding the six balanced functions f_3–f_8 are implemented by selective pulses on the transitions of the control qubit, taken two at a time, i.e., the pulses can be described by $[\pi,\pi,0,0]$, $[\pi,0,\pi,0]$, $[\pi,0,0,\pi]$, $[0,\pi,\pi,0]$, $[0,\pi,0,\pi]$, and $[0,0,\pi,\pi]$ on the four transitions, where 0 denotes no pulse on that particular transition. The phases of the transition selective pulses have been stepped through $(x,-x,y,-y)$ as in the two-qubit case, and a similar logic prevails in explaining the spectral pattern obtained. Unlike the previous implementation of the three-qubit DJ algorithm [19], the phase cycling here achieves a complete suppression of the multiplets of both the target spins when the function is balanced $(f_3$–$f_8)$.

It has been demonstrated that selective pulse techniques in NMR are a powerful tool to build quantum information processors. The distilling of a pseudopure state from a thermal state, the simultaneous implementation of different logical operations to save computational time, and a two- and three-qubit implementation of the DJ quantum algorithm has been experimentally achieved using such techniques.

ACKNOWLEDGMENTS

The use of the AMX-400 high resolution FTNMR spectrometer of the Sophisticated Instruments Facility, Indian Institute of Science, Bangalore, funded by the Department of Science and Technology, New Delhi, is gratefully acknowledged.

[1] I.L. Chuang, R. Laflamme, P.W. Shor, and W.H. Zurek, Science **270**, 1633 (1995).
[2] D.P. DiVincenzo, Science **270**, 255 (1995).
[3] R.P. Feynmann, Int. J. Theor. Phys. **21**, 467 (1982).
[4] D. Deutsch, Proc. R. Soc. London, Ser. A **425**, 73 (1989).
[5] A. Barenco, C.H. Bennett, R. Cleve, D.P. DiVincenzo, N. Margolus, P. Shor, T. Sleator, J.A. Smolin, and H. Weinfurter, Phys. Rev. A **52**, 3457 (1995).
[6] D.P. DiVincenzo, Phys. Rev. A **51**, 1015 (1995).
[7] P.W. Shor, SIAM J. Comput. **26**, 1484 (1997).
[8] D. Deutsch and R. Jozsa, Proc. R. Soc. London, Ser. A **439**, 553 (1992).
[9] L.K. Grover, Phys. Rev. Lett. **79**, 325 (1997).
[10] J.I. Cirac and P. Zoller, Phys. Rev. Lett. **74**, 4091 (1995).
[11] D.G. Cory, A.F. Fahmy, and T.F. Havel, Proc. Natl. Acad. Sci. USA **94**, 1634 (1997).
[12] E. Knill, I.L. Chuang, and R. Laflamme, LANL preprint, quant-ph/9706053.
[13] N. Gershenfeld and I.L. Chuang, Science **275**, 350 (1997).
[14] I.L. Chuang, L.M.K. Vandersypen, X. Zhou, D.W. Leung, and S. Lloyd, Nature (London) **393**, 143 (1998).
[15] I.L. Chuang, N. Gershenfeld, and M. Kubinec, Phys. Rev. Lett. **80**, 3408 (1998).
[16] I.L. Chuang, N. Gershenfeld, M.G. Kubinec, and D.W. Leung, Proc. R. Soc. London, Ser. A **454**, 447 (1998).
[17] J.A. Jones and M. Mosca, J. Chem. Phys. **109**, 1648 (1998).
[18] J.A. Jones, R.H. Hansen, and M. Mosca, J. Magn. Reson. **135**, 353 (1998).
[19] N. Linden, H. Barjat, and R. Freeman, Chem. Phys. Lett. **296**, 61 (1998).
[20] Z.L. Madi, R. Bruschweiler, and R.R. Ernst, J. Chem. Phys. **109**, 10 603 (1998).
[21] Lieven M.K. Vandersypen, C.S. Yannoni, M.H. Sherwood, and I.L. Chuang, LANL e-print quant-ph/9905041.
[22] Kavita Dorai and Anil Kumar, J. Magn. Reson., Ser. A **114**, 155 (1995).
[23] Lewis Carroll, *Through the Looking Glass and What Alice Found There* (Hamlyn House, Feltham, Middlesex, 1871).
[24] R. R. Ernst, G. Bodenhausen, and A. Wokaun, *Principles of Nuclear Magnetic Resonance in One and Two Dimensions* (Clarendon Press, Oxford, 1987).
[25] D.G. Cory, A.E. Dunlop, T.F. Havel, S.S. Somaroo, and W. Zhang, LANL e-print quant-ph/9809045.